European Journal of Pharmaceutics and Biopharmaceutics 160 (2021) 143–151

Contents lists available at ScienceDirect

European Journal of Pharmaceutics and Biopharmaceutics

journal homepage: www.elsevier.com/locate/ejpb

Novel insights on the encapsulation mechanism of PLGA terminal groups on ropivacaine

Xun Li [a,b], Yi Wei [a,*], Kang Wen [a,b], Qingzhen Han [c], Kenji Ogino [d], Guanghui Ma [a,*]

[a] State Key Laboratory of Biochemical Engineering, PLA Key Laboratory of Biopharmaceutical Production & Formulation Engineering, Institute of Process Engineering, Chinese Academy of Sciences, Beijing 100190, PR China
[b] University of the Chinese Academy of Sciences, Beijing 100049, PR China
[c] State Key Laboratory of Multiphase Complex Systems, Research Department for Environmental Technology and Engineering, Institute of Process Engineering, Chinese Academy of Sciences, Beijing 100190, PR China
[d] Graduate School of Bio-Applications Systems Engineering, Tokyo University of Agriculture and Technology, Koganei, Tokyo 184-8588, Japan

ARTICLE INFO

Keywords:
Terminal groups
Ropivacaine
Specific interactions
Pharmacokinetics
Pharmacodynamic

ABSTRACT

Currently, the influences of free terminal groups (hydroxyl, carboxyl and ester) of PLGA on encapsulating active pharmaceutical ingredient are relatively ambiguous even though PLGA types were defined as critical quality attributes in vast majority of design of experiment process. In this study, emulsion method combined with premix membrane emulsification technique has been used to encapsulate ropivacaine (RVC), a small molecule local anesthetic in clinical. Based on the narrow particle size distribution, the influences and mechanisms of the terminal groups on properties of ropivacaine loaded microspheres have been investigated in detail. It was found that microspheres prepared by PLGA with hydroxyl or ester groups exhibited lower encapsulation efficiency but faster *in vitro* release rate than that of carboxyl groups. In the meanwhile, on microcosmic level analysis by quartz crystal microbalance with dissipation, atomic force microscope and confocal laser scanning microscopy, we attributed this distinction to the specific interaction between ropivacaine and different terminal groups. Subsequently, the reaction activation centers were verified by density functional simulation calculation and frontier molecular orbital theory at molecular level. Additionally, pharmacokinetics and pharmacodynamic research of infiltration anesthesia model were performed to compare sustained release ability, duration and intensity of the anesthetic effect *in vivo*. Finally, potential safety and toxicity were evaluated by the biochemical analysis. This study not only provides a novel mechanism of drug encapsulation process but also potential flexible selections in terms of various anesthesia indications in clinical.

1. Introduction

19 different long-acting injectable depot formulations based on poly (lactic-co-glycolic acid) (PLGA) have been applicated clinically since 1989. As synthetic aliphatic polyesters of hydroxyl acids materials approved by the Food and Drug Administration (FDA), PLGA possesses remarkable biocompatibility and eventually hydrolyzed to carbon dioxide and water [1]. Generally speaking, depending on the molecular weight and lactide:glycolide ratio, PLGA as polymer matrix which provides a tailored biodegradation rate from days to months could meet the indication requirement and administration regimen in clinical.[2–4]. Therefore, PLGA types were normally identified as critical process parameters (CPP) in design of experiment (DOE) process. Moreover, except for different molecular weight and the copolymer ratio, the type of PLGA could also be characterized as hydroxy terminal group (PLGA-OH), carboxyl-terminal group (PLGA-COOH) and ester terminal group (PLGA-COOR) based on the available free terminal groups [5]. Till now, there are several literatures reported that terminal groups could induce the distinction in characteristics of polymer, which may further affect the property of microspheres, especially on the encapsulation efficiency % and release kinetics. More specifically, Maria found that the carboxyl-terminal groups lead to a higher drug loading efficiency than ester-terminal group when encapsulating L-asparaginase into microsphere [6]. Lam found that rhIGF-I encapsulated by free carboxyl-terminal groups gave rise to relative lower initial burst and more steady-state release profile than the ester-terminal groups with the same protein loading and PLGA molecular weight [7]. It is worth mentioning that above relevant research only reported the phenomenon itself and did not

* Corresponding authors.
E-mail addresses: ywei@ipe.ac.cn (Y. Wei), ghma@ipe.ac.cn (G. Ma).

https://doi.org/10.1016/j.ejpb.2021.01.015
Received 18 May 2020; Received in revised form 25 December 2020; Accepted 23 January 2021
Available online 30 January 2021

further dig out the understanding of mechanism. This is partly because the broad particle size distribution produced by the conventional preparation method will lead to a poor repeatability. Another reason for that is there are a variety of groups in the encapsulated biomolecules which will induce interference.

In this study, ropivacaine, a small molecule local anesthetic widely used in clinical [8], has been chosen as model drug. Due to its hydrophobic properties, ropivacaine loaded microsphere with different PLGA terminal groups were prepared through the O/W emulsion method combined with a premix membrane emulsification technique [9]. The narrow size distribution eliminated the poor reproducibility and guaranteed resulting credibility [10]. Subsequently, systematic evaluation of ropivacaine loaded microsphere was performed, including morphology, encapsulation efficiency and *in vitro* release behavior. Furthermore, the specific interaction between drug and polymer as well as the microenvironment *pH* change during microsphere degradation process were explored on microcosmic level. In the meantime, Density Functional and Frontier Molecular Orbits Calculations were calculated to analyze the reaction activation centers and interaction mechanism at molecular level. In addition, pharmacokinetics experiment expressed the sustained release ability of microsphere *in vivo*. The duration and intensity of the anesthetic effect were evaluated by the block of Cutaneous Trunci Muscle Reflex (CTMR) using a model of infiltration anesthesia [11,12]. Eventually, the potential cardiotoxicity of ropivacaine loaded microsphere was investigated by biochemical analysis.

2. Materials and method

2.1. Materials

PLGA with number-average molecular weights (*Mn*) of 10000, mol ratio of d,l-lactide/glycolide 50/50, terminal groups of COOH, OH, COOR respectively, were supplied by the Dai Gang company (Shandong, China). The *Mn* and *Mw/Mn* values of PLGA were obtained with gel permeation chromatography (GPC, Waters, USA) using polystyrene as a standard. Poly vinyl alcohol (PVA-217, degree of polymerization 1700, degree of hydrolysis 88.5%) was provided by Kuraray (Japan). The SNARF-1-AM dextran fluorescent *pH*-sensitive dye (Mw = 10 kDa) was from Molecular Probes (USA). Ropivacaine base was provided by Humanwell Pharmaceutical Co., Ltd. (Hubei, China). Premix Membrane Emulsifier (FM0210/500 M) and microporous membrane (pore size of the membrane was 35 μm) were provided by Senhui Microsphere Tech (Suzhou) Co., Ltd. All other reagents were of analytical grade.

2.2. Preparation of microspheres

Ropivacaine loaded microspheres were prepared by premix membrane emulsification technique combined with oil-in-water (O/W) emulsion method as our previous study reported [13]. Briefly, ropivacaine base (400 mg) and PLGA (600 mg) were dissolved into dichloromethane (DCM) (5 mL), which was employed as oil phase(O). The oil phase (O) was subsequently emulsified into 100 mL 1% PVA solution (W) by homogenizer at 3000 rpm to form coarse emulsion of O/W. Then, the coarse emulsion were transferred into the storage tank of premix membrane emulsification equipment, which were repeatedly pressed through the pore (35 μm) of membrane under proper pressure to obtain uniform-sized emulsion droplets. After that, the emulsion were solidified under vacuum pressure by rotary evaporator for 6 min. At last, the microspheres were collected by centrifugation, washed with distilled water for 5 times and obtained after freeze-drying.

2.3. Surface morphology observation and size distribution measurement

The shape and surface morphology of microspheres were observed by a JSM-6700F (JEOL, Japan) scanning electron microscope (SEM). Particle size distribution was measured by laser diffraction using Mastersizer 2000 (Malvern, UK). It was referred to as Span value and calculated as follows:

$$\text{Span} = \frac{D_{V,90\%} - D_{v,10\%}}{D_{v,50\%}}$$

where *Dv,90%*, *Dv,50%* and *Dv,10%* are volume size diameters at 90%, 50% and 10% of the cumulative volume, respectively. The smaller Span value indicates the narrower size distribution.

2.4. Loading efficiency % (LE%) and encapsulation efficiency % (EE%) measurement

Ropivacaine loaded microspheres (10 mg) were dispersed in 5 mL acetonitrile and vigorously vortexed for 10 min. The concentration of ropivacaine was determined by high-performance liquid chromatography (HPLC) using a Syncronis C18 (250 mm × 4.6 mm × 5 mm, Thermos) chromatographic column at room temperature. Linear gradient elution was performed from 50% acetonitrile–phosphate buffer (pH = 8.0) for 15 min. The flow rate was 1 mL/min. UV absorbance was 240 nm. The drug loading efficiency (LE%) and encapsulation efficiency (EE%) of the microspheres were calculated by the following equations:

$$\text{LE} = \frac{a}{b} \times 100\%$$

where b is the total mass of microspheres (including the mass of polymer and ropivacaine loaded) and a is the mass of ropivacaine loaded in the microspheres.

$$\text{EE} = \frac{m}{m_0} \times 100\%$$

where m_0 is the total mass of ropivacaine added and m is the mass of ropivacaine loaded in the microspheres.

2.5. In vitro release study

Ropivacaine loaded microspheres (10 mg) prepared by the different terminal groups were incubated in 1 mL of phosphate buffer saline (PBS) containing 0.1% Tween 80 and 0.1% Tween 20 medium (pH 7.4) under agitation at 37 ℃. At each predetermined interval, supernatants were collected by centrifugation and replaced with a fresh buffer of equal volume. The concentration of ropivacaine in the supernatant was determined by HPLC. All the release experiments were executed in triplicate.

2.6. Quartz crystal microbalance with dissipation (QCM-D) measurement

The quartz crystal microbalance (QCM-D) technique is widely used to measure the real-time molecule adsorption in liquid-phase research applications [14,15]. Investigating the adsorption quantity of terminal group PLGA films can reflect the interaction between the different terminal groups of PLGA and ropivacaine. The principle of QCM-D is to apply an ac voltage in the megahertz range across an AT-cut piezoelectric quartz crystal and to record the resonance frequency of the crystal 250 mg of PLGA (PLGA-OH, PLGA-COOR, and PLGA-COOH) were dissolved in 5 mL of ethyl acetate to obtain a polymer solution. The polymer solution was cast on an Au-coated sensor crystal and coated with a spin coater at a speed of 5000 rpm for 60 s. The PLGA film was air-dried first and then completely dried in a vacuum oven. The ropivacaine hydrochloride was dissolved in water as adsorption solution. The QCM-D experiments were coupled to a peristaltic pump using a flow rate of 50 μL/min and conducted at 23 °C. When the adsorption of ropivacaine reached saturation at a particular concentration, degassed buffer (acetic acid aqueous solution, pH 4.2) was injected into the chamber to desorb ropivacaine using a flow rate of 150 μL/min until the balance was achieved.

2.7. Atomic force microscope (AFM) measurement

The adsorption ability of different terminal groups can be reflected by the topographical changes in the PLGA film surface [16]. After ropivacaine adsorption and subsequent desorption by QCM-D, the topographical changes in the PLGA film surface were observed by atomic force microscopy (Multimode AFM, Veeco Co, Ltd., USA) at 25 °C. The AFM images were obtained in the Scanasyst-in-air mode with a silicon nitride cantilever at a scanning speed of 1.0 Hz and a scanner with maximum ranges of 5 μm in the × and *y* directions and 10 nm in the *z* direction. A 3D sample surface can be imaged by scanning a film surface with the probe tip at a constant interaction. A commercial AFM image-processing software package, Nanoscope 8.1 from Veeco was used. Roughness data were obtained from a minimum of three separate images of different regions on each sample.

2.8. Confocal imaging of the microclimate pH inside microspheres

The microclimate *pH* inside microspheres over incubation was monitored by laser scanning confocal microcosmic imaging. In brief, 0.5 mL 3 to 4 mg/mL SNARF-1-AM dextran (fluorescent *pH*-sensitive dye) was added to 5 mL of DCM together with PLGA and ropivacaine to form the oil phase. The other procedures were as same as in method 2.2. 10 mg of microspheres were suspended in 1 mL of PBS buffer (pH 7.4) under mild agitation at 37 °C. After a predetermined interval, microspheres encapsulated with fluorescent *pH*-sensitive dye were observed for the microclimate pH change. The fluorescent dye was excited at 488 nm by an Ar/He laser, and two images at different wavelengths (580 and 640 nm) were taken. The two images were overlapped to observe the microclimate pH change. The dye shows red light (pH close to 6.0) and green light (pH close to 9.0), when the dye shows yellow, the pH is close to neutrality. [17,18]. Additionally, the ratio of the fluorescence intensities from the dye at two emission wavelengths (640 and 580 nm) is used to analyze *μpH* quantitatively, and the lower value indicates the more acidic *pH*.

2.9. Density functional and frontier molecular Orbits Calculations

Density functional theory (DFT) is a theory to study the ground-state properties of multi-particle systems by using electron density distribution (p(r) as a basic variable. It is widely used in thermodynamic studies of chemical reaction processes. Molecular structure, charge distribution can be predicted by calculating the activation energy, free energy, and chemical reaction path. In this case, the B3LYP method of density functional theory (DFT) is used to optimize the structure at the level of 6-311G (d, P) basis set level. The frequency analysis of the optimized structure showed that there was no imaginary frequency. The structure exhibited a stable configuration characteristic. Subsequently, the charge distribution of activated center atoms of ropivacaine and PLGA units with different terminal groups and frontier molecular orbit were calculated. The structural optimization was carried out at the same level, and all calculations were completed by using the gaussian 09 program package.

2.10. Pharmacokinetic analysis

Twenty-four Male Sprague-Dawley rats weighing about 200–300 g were used to investigate the pharmacokinetics study. Animals were housed three per cage with controlled relative humidity (20%–30%) in a 12-hour light–dark cycle at room temperature (24 °C). Food and water were freely accessed. Rats were divided into four groups at random and administrated via subcutaneous single 2 mg/kg dose of the ropivacaine on both formulations (ropivacaine loaded microsphere and plain ropivacaine solution). Blood samples (0.3 mL) were collected into heparinized tubes from the jugular vein at 0.5, 1, 2, 4, 8, 12, 24, 48, 72, and 96 h after subcutaneous administration. Blood was immediately processed for plasma by centrifugation at 3,500 × g for 10 min. The plasma samples were kept at − 70 °C. The plasma concentration of RVC was measured by high-performance liquid chromatography-mass spectrometry, which was performed on a LC-10A system (Shimadzu, Kyoto, Japan), equipped with a Welch XB C18 column (3 μm, 2.1 × 50 mm). The detection wavelength was set at 215 nm, and the mobile phase solvent consisting of methanol and 5 mM Ammonium format buffer was pumped at a flow rate of 0.3 mL/min. Bupivacaine hydrochloride was used as an internal standard. MS detection: The analytes were detected in the positive electrospray ionization mode with multiple reactions monitoring (MRM). The ESI source values were as follows: capillary voltage,3.50 kV; source temperature, 150℃; desolvation temperature, 500℃; desolvation gas (nitrogen, 99.99% purity) flow, 1000 L/h. The MRM transitions monitored were *m/z* for parent ion 275.2 & daughter ion 126.0 (Ropivacaine), *m/z* for parent ion 289.2 & daughter ion 140.2 (Bupivacaine). After method validation, it is determined that the linearity range of ropivacaine is 5 ng/mL-1000 ng/mL. The LOQ of ropivacaine is 1 ng/mL Pharmacokinetics parameters were calculated using the non-compartment model analysis (NCA) of WinNonlin 6.4.

2.11. Pharmacodynamic evaluation

Infiltrative cutaneous analgesia model was used to estimate pharmacodynamic study. The Male Sprague-Dawley rats weighing about 200–300 g were used in the pharmacodynamic study. Animals were housed three per cage with controlled relative humidity (20%–30%) in a 12-hour light–dark cycle at room temperature (24 °C). Food and water were freely accessed. The hair on the dorsal region of the animals' thoracolumbar area (6 cm × 8 cm) was shaved before injection. As a characteristic response to a noxious pinprick, the Cutaneous Trunci Muscle Reflex (CTMR) was investigated. It is defined as the reflex movement of the skin over the back generated by convulsive movements of lateral thoracic-spinal muscles as a consequence of a local stimulus [19,20]. Inhibition of CTMR was utilized as a model of infiltration anesthesia, according to the literature [21]. Ropivacaine loaded microspheres containing 10 mg ropivacaine and 2 mg plain ropivacaine solution were administered subcutaneously in 0.6 mL saline solution. The injections produced a round wheal (about 2 cm) of the skin, that was delineated with ink within the 30 s. Six pinpricks were then applied inside this zone, and the number to which the rat failed to respond was measured. The intensity of the local anesthetic effect was calculated quantitatively as the number of times the stimulus failed to induce a CTMR response and was described as the percentage of possible effect (%PE) [20]. For example, the complete absence of six responses demonstrated to be a full nociceptive block (100% of possible effect; 100% PE), which was calculated as follows:

$$\%PE = ((\text{number of stimuli that elicited no response})/6) \times 100\%$$

Measurements (6 pinpricks each) were performed at preset time intervals (0.5 h、2h、4h、6h、8h、10 h、12 h、14 h、16 h、18 h、20 h、22 h、24 h) up to a full recovery was attained. All formulations were solubilized or suspended in saline. The saline was used as a control group. Blank microsphere group was administered at the same concentration as in the corresponding drug-loaded formulation. Behavioral measurements were performed on 6 rats for each treatment.

2.12. Biochemical analysis

In order to investigate the potential cardiotoxicity of ropivacaine loaded microspheres, rat serum was collected after pharmacodynamic evaluation and biochemical analyses were performed. The indicators such as aspartate transaminase (AST) and lactate dehydrogenase (LDH) which can reflect the cardiac toxicity were determined. All analyses were carried out using the Analyzer Medical System (AUTO LAB, Italy).

3. Results and discussion

3.1. Characterization of microspheres

Uniform-sized ropivacaine loaded microspheres with high theoretical drug loading efficiency (40%) were successfully prepared by different terminal groups of PLGA for comparison. As shown in Fig. 1, smooth surface and regular sphericity were observed for all microspheres. The particles size of ropivacaine loaded microspheres (OH-RVC-MS, COOH-RVC-MS and COOR-RVC-MS) fabricated respectively by PLGA with OH, COOH and COOR terminal groups were all around 17 μm (Fig. S1). It was worth mentioning that the narrow size distribution guaranteed the good reproducibility and reliability of the following research. As shown in Table 1, the 94.6% of EE% was obtained by using PLGA with the COOH terminal group, as compared to 83.8% with the OH terminal group and 80.5% with the COOR terminal group. It was discovered that the terminal groups of PLGA exercise significant effect on ropivacaine incorporation and content in the microspheres.

3.2. In vitro release profile

In vitro release profiles of all groups were compared based on the similar particle size. As Fig. 2 exhibited, OH-RVC-MS, COOH-RVC-MS, COOR-RVC-MS showed an initial burst release of 11.1%, 3.8%, 15.9% over the first 1 h, respectively. With incubation proceeded, approximate 67.3% of ropivacaine was released in 8 days from PLGA-COOH-MS, while 85.3% and 89.5% of ropivacaine have been released in 4 days from PLGA-OH-MS and PLGA-COOR-MS. It can be found that the release behavior of three groups were totally different. To be specific, COOH-RVC-MS exhibited much slower release rate than OH-RVC-MS and COOR-RVC-MS groups, whether initial burst phase or average release rate.

We attributed the obvious distinction of encapsulation efficiency and *in vitro* release behavior to the specific interactions between the polymer and drug which might caused by the different terminal groups. Moreover, the difference mechanism of release rate could be illustrated in Sections 3.3 and 3.5.

3.3. The interactions between ropivacaine and PLGA

In order to confirm our hypothesis, the interactions between terminal groups and ropivacaine have been quantitatively analyzed by QCM-D and AFM. In this section, films made of PLGA with different end groups were used for reflecting the polymer themselves. Hence, after absorption and desorption process, the interactions between PLGA and ropivacaine can be reflected by the residual adsorption quantity. Firstly, ropivacaine adsorbed on the surfaces of PLGA films were detected by QCM-D. Two parameters, frequency (F) and dissipation (D), were monitored during the whole adsorption and desorption process. The mass changes in films can be reflected by frequency fluctuation. A decrease in frequency meant an increase in film mass. In the meanwhile, the structural variations in thin viscoelastic films can be characterized by measuring the dissipation. The enhancement of dissipation indicated that the structure of the film became rough. Fig. 3 showed the changes in frequency (ΔF) and dissipation (ΔD) for a different terminal groups of PLGA film during the adsorption and subsequent desorption process. As shown in Fig. 3A, PLGA-COOH resulted in a decrease in frequency (ΔF) of 41.5 Hz and an increase in dissipation (ΔD) of 5.96. For PLGA-OH and PLGA-COOR ones (Fig. 3B, C), smaller decrease in frequency (10.16 and 0.24 Hz, respectively) and smaller increases in dissipation (3.89 and 0.26, respectively) were observed. These results demonstrated that PLGA-COOH can absorb more ropivacaine than PLGA-OH and PLGA-COOR.

Furthermore, we observed the topographical changes after desorption of ropivacaine by QCM-D. Fig. 4 and SI-Table 1 showed that the amount of ropivacaine adsorbed on the surface of PLGA-COOH was much larger than that of PLGA-OH and PLGA-COOR. This experiment phenomenon also identified the results of the QCM-D test. Therefore, it can be concluded that the different terminal groups of PLGA lead to different absorption ability to ropivacaine. Moreover, it also illustrated the distinction in critical quality attributes of ropivacaine microsphere prepared by PLGA with different end groups.

Table 1
Characterization of OH-RVC-MS, COOH-RVC-MS and COOR-RVC-MS (Results are Mean ± Standard Deviation (SD), n = 3).

	Average diameter/ μm	Span	LE%	EE%
OH-RVC-MS	17.01 ± 0.67	0.527	33.52 ± 0.87	83.8 ± 2.03
COOH-RVC-MS	17.15 ± 0.38	0.553	37.84 ± 1.23	94.6 ± 3.075
COOR-RVC-MS	17.49 ± 0.71	0.538	32.2 ± 0.49	80.5 ± 1.23

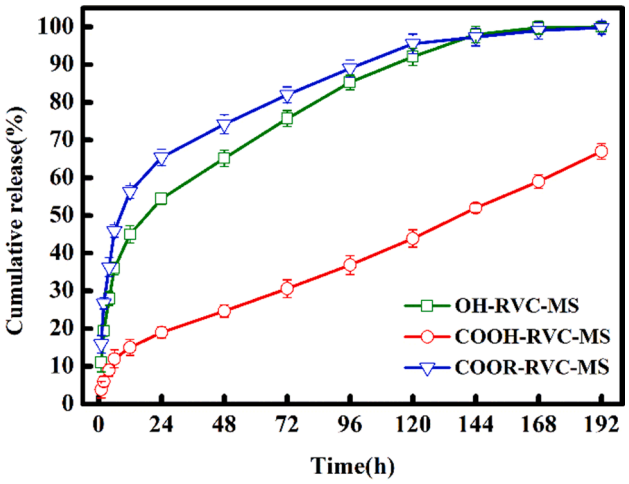

Fig. 2. In vitro cumulative release profiles (n = 3, mean ± SD).

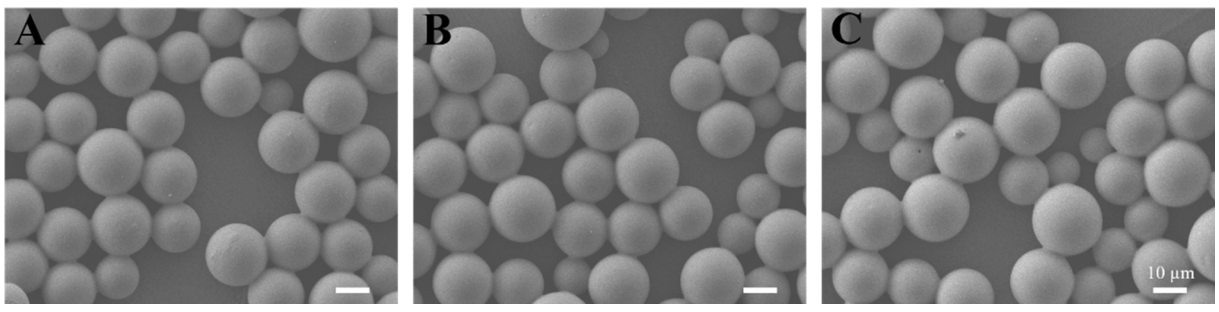

Fig. 1. SEM images of OH-RVC-MS, COOH-RVC-MS and COOR-RVC-MS.

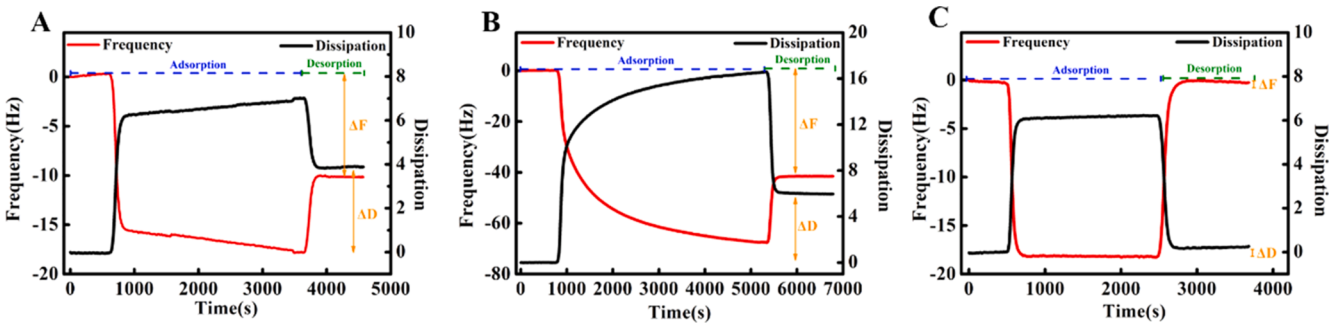

Fig. 3. Diagram of frequency (red line) and dissipation (black line) vs time for exposure of the (A) PLGA-OH, (B) PLGA-COOH, and (C) PLGA-COOR surfaces to ropivacaine solution, followed by the exchange of the ropivacaine solution with buffer solution. ΔF and ΔD represent the changes in frequency and dissipation, respectively when desorption becomes saturated.

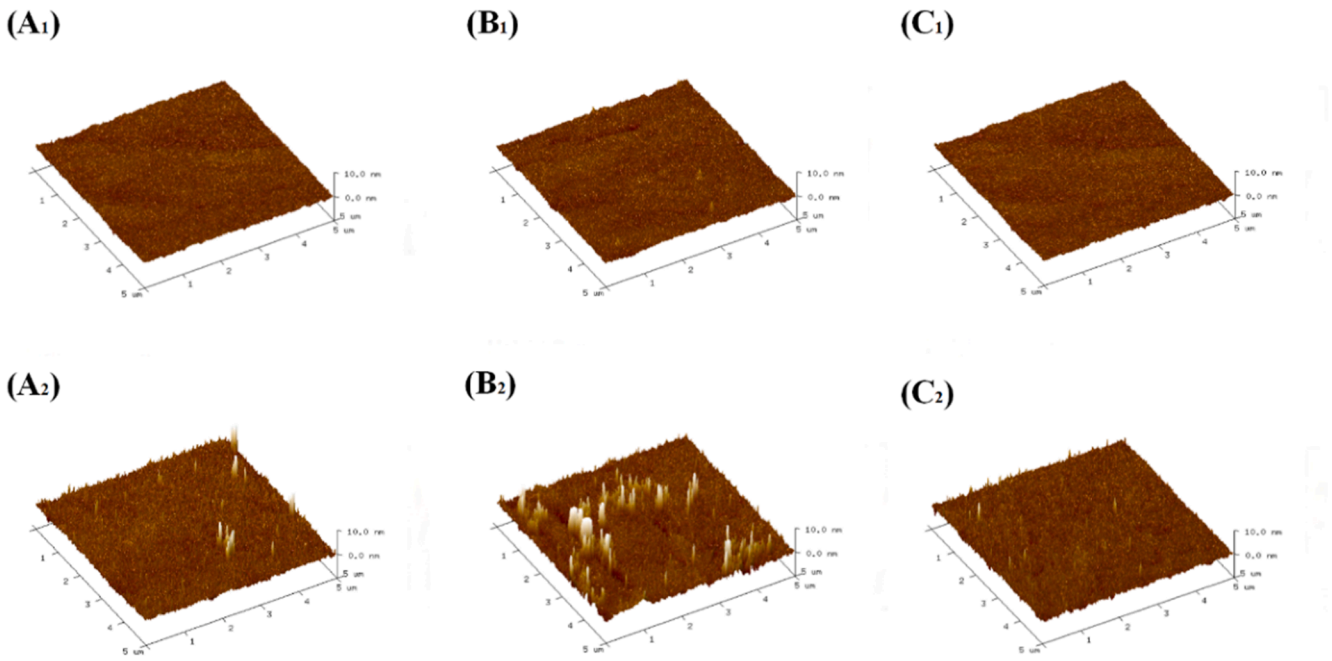

Fig. 4. AFM images of PLGA films: before adsorption: (A_1) PLGA-OH, (B_1) PLGA-COOH, and (C_1) PLGA-COOR;after the adsorption and subsequent desorption: (A_2) PLGA-OH, (B_2) PLGA-COOH, and (C_2) PLGA-COOR.

3.4. Microclimate pH in microspheres

In order to further explore the mechanism of the release process, the microenvironment created inside the microspheres with the different terminal group was investigated. As shown in Fig. 5, RVC-OH-MS and RVC-COOR-MS presented light green, while RVC-COOH-MS exhibited light orange at first 24 h. It indicated that the microenvironment of RVC-COOH-MS was much more acidic than that of RVC-OH-MS and RVC-COOR-MS at first 24 h. Additionally, the quantitative analysis of μpH changes during the incubation times was also calculated by the ratios of fluorescence intensities measured at two wavelengths (I640/I580). As shown in Fig. S2, RVC-COOH-MS exhibited lower values (I640/I580) than RVC-OH-MS and RVC-COOR-MS during the whole incubation, implying that the *μpH* inside RVC-COOH-MS was more acidic. This phenomenon might be attribute to the terminal carboxyl groups of PLGA interacted with the amino group of ropivacaine, which acted to neutralize the alkaline of the ropivacaine base. Whereas the terminal hydroxy groups and terminal ester groups of PLGA could not interact with the amino group of ropivacaine, thus the microenvironment of RVC-OH-MS and RVC-COOR-MS mainly dominated by the weak alkaline of the ropivacaine base. With incubation proceeding, the RVC-OH-MS and RVC-COOR-MS turned into yellow gradually, suggesting the microenvironment became neutral. The RVC-COOH-MS turned into dark orange which meant the microenvironment got acidic. Simultaneously, as shown in Fig.S2, the decreased ratio values (I640/I580) of three groups were also quantificationally indicate the change of microenvironment.

3.5. Density functional theory calculation and frontier molecular orbits analysis

The interaction between PLGA and ropivacaine with different terminal groups were quantitatively characterized at the micro-level in above research. The results showed that, for ropivacaine molecule, the absorption ability of the carboxylic terminal was greater than that of the hydroxyl terminal and ester terminal groups. In this section, the specific interaction was identified at the molecular level. The reaction activation centers in each molecule are analyzed by density functional theory and frontier molecular orbital theory. In the theory of frontier orbital, chemical reactions occur in the positions and directions where the highest occupied orbital (HOMO) of one reactant and the lowest empty orbital (LUMO) of another reactant could generate overlap maximumly. The closer energy of HOMO and LUMO involved in the reaction represented stronger interaction between the representative and more stable

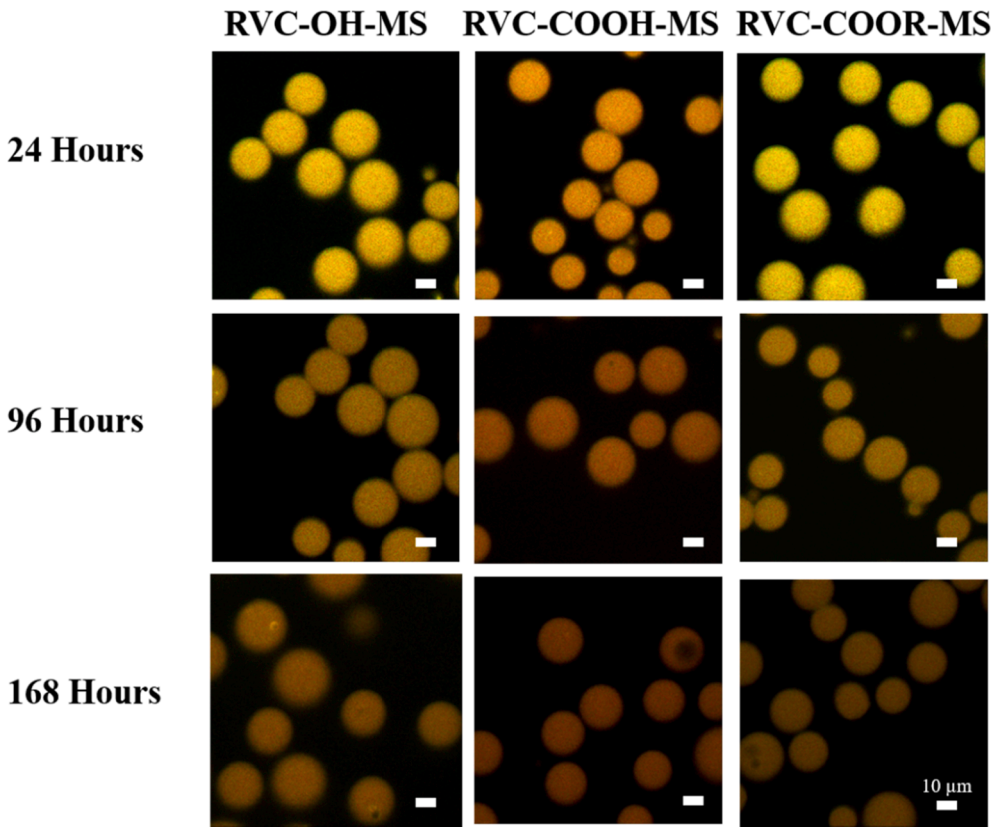

Fig. 5. CLSM images of *pH*-sensitive dye-loaded microspheres with different terminal groups at different incubation times (24, 96, and 168 h). The scale bar is 10 μm.

system. Furthermore, in the principle of molecular orbital symmetry, reactions are prone to occur when HOMO and LUMO symmetry match, while reactions are difficult to occur when they do not match.

As shown in Fig.S2 and Table 2, in the bonding process, electrons are transferred from the HOMO to the LUMO of the reaction centers. According to the energy analysis of frontier orbital theory, ropivacaine molecule has the highest energy of HOMO (-0.23367). Hence, the intermolecular bonding process mainly generated through the electrons transfer from the HOMO of ropivacaine to LUMO of PLGA. Subsequently, the reaction activation centers of ropivacaine and PLGA with different terminal groups were determined according to the charge density distribution and steric hindrance principle.

As shown in Fig. 6, in ropivacaine molecule, N atom (-0.410) in the hexatomic ring acted as hydrogen bond acceptor, while in terminal groups of PLGA, H atom (0.261) at alpha position of OH-PLGA, H atom (0.286) at alpha position of COOH-PLGA, and H atom (0.269) at beta position of COOR-PLGA acted as hydrogen bond donor respectively. The hydrogen bond receptor bonded to the donor, and the order of magnitude of charge represent the order of strength of binding. Therefore, COOH-PLGA had the strongest binding ability to N atom in ropivacaine. Additionally, the binding ability of COOR-PLGA was slight stronger than OH-PLGA. However, the binding ability of PLGA with N atom in ropivacaine was strictly restricted due to the large steric hindrance of ester terminal groups. Hence, OH-PLGA exhibited stronger binging ability than COOR-PLGA. In conclusion, the above experimental phenomena were verified by the density functional simulation calculation and frontier molecular orbital theory at the molecular level.

Table 2
Frontier molecule orbital energy of different PLGA terminal group units and ropivacaine.

Molecule unit	E_{HOMO}	E_{LUMO}
RVC	−0.23367	−0.02073
OH-PLGA	−0.28224	−0.01954
COOH-PLGA	−0.27920	−0.01680
COOR-PLGA	−0.28211	−0.01669

3.6. Pharmacokinetic study

The plasma concentration–time profiles were shown in Fig. 7. It was found that the ropivacaine loaded microspheres prepared by different terminal group exhibited different release behaviors *in vivo*. The OH -RVC-MS, the COOH -RVC-MS and the COOR-RVC-MS achieved maximal plasma concentrations (78.09 ± 13.9 ng/mL, 12.92 ± 1.3 ng/mL and 81.23 ± 18.2 ng/mL), which were significantly lower than that of the plain ropivacaine solution group (181.92 ± 23 ng/mL). Additionally, the OH -RVC-MS and the COOR -RVC-MS group exhibited a higher initial burst *in vivo*, which consistent with the *in vitro* release behaviors.

Furthermore, pharmacokinetic parameters were shown in Table 3. The elimination half-life time ($T_{1/2}$) (0.82 h) and Mean Residual Time (MRT) (1.2 h) of ropivacaine hydrochloride solution group were shorter than that of all microsphere's groups, suggesting that the ropivacaine loaded microspheres formulation could significantly prolong the release behavior *in vivo*. While the microspheres prepared by different terminal groups were compared in further, it was found that the area under the concentration–time curve (AUC) value of COOH -RVC-MS (102.14 ng·h/mL) were lower than that of OH -RVC-MS (442.18 ng·h/mL) and COOR -RVC-MS (471.09 ng·h/mL), this phenomenon might be attributed to the slow release rate caused by strong interaction between COOH terminal groups and ropivacaine. Hence, considering the sustain release ability along with bioavailability, the formulation of OH -RVC-MS could be chosen as a priority.

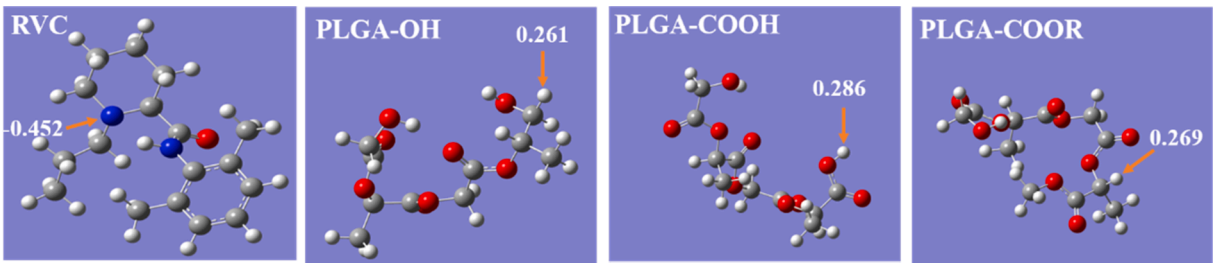

Fig. 6. Reaction activation center of Ropivacaine and PLGA.

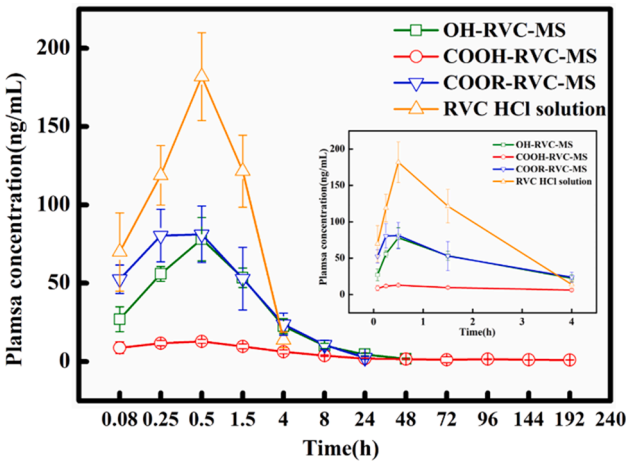

Fig. 7. Plasma ropivacaine concentration vs. time profiles of OH-RVC-MS, COOH-RVC-MS, COOR-RVC-MS and plain RVC solution (n = 6, mean ± SD).

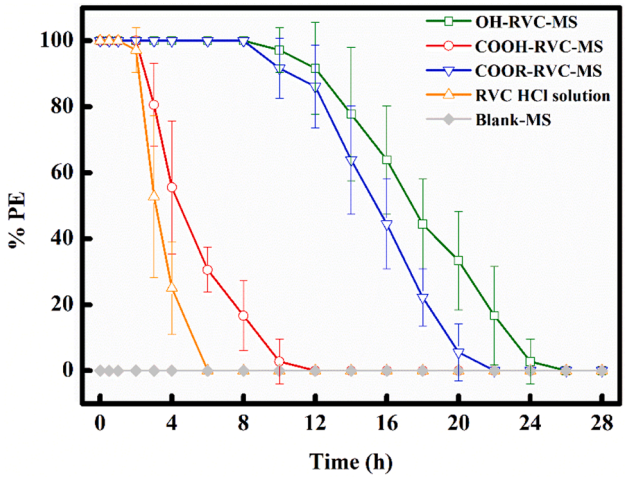

Fig. 8. Normalized mean (±SEM) degree of anesthetic effect (expressed as % of possible effect) versus time curve achieved by Cutaneous Trunci Muscle Reflex (CTMR) test.

Table 3
Pharmacokinetic parameters of different formulations of ropivacaine.

Formulations	$T_{1/2}$ (h)	C_{max} (ng/mL)	AUC (ng·h/mL)	MRT (h)
OH-RVC-MS	15.81	78.09	442.18	14.98
COOH-RVC-MS	12.83	15.92	102.14	16.78
COOR-RVC-MS	6.12	81.23	471.09	6.96
RVC HCl solution	0.82	181.92	381.90	1.20

Note: Each parameter represents the mean ± SD of 6 rats.

3.7. Pharmacodynamic evaluation

As displayed in Fig. 8, the ropivacaine loaded microspheres groups and ropivacaine solution presented the anesthesia effect compared with blank microsphere group. Furthermore, the influences of terminal group on pharmacodynamic have also been compared. It could be found that the OH-RVC-MS group exhibited the best therapeutic efficacy, in terms of both intensity and duration of anesthetic effect. The COOH-RVC-MS group showed relative weaker anesthetic effect, this was because of the stronger interaction between PLGA and ropivacaine will lead to a slow- release behavior. Hence, the low concentration of ropivacaine was difficult to reach an effective dose.

3.8. Biochemical analysis

Ropivacaine has a considerable side effect on the cardiovascular system when accidentally injected intravascularly or administered in excessive doses [22]. This is because the combination of ropivacaine and Na^+ channel-specific sites in cardiomyocytes blocks the Na^+ channel of myocardial cell membranes, causing damage to myocardial cell membrane structure and release of myocardial enzymes, which leads to the increase of AST, LDH [23,24]. Therefore, the potential cardiotoxicity of ropivacaine loaded microsphere was evaluated by biochemical analysis. As shown in Fig. 9, the LDH and AST of COOH-RVC-MS group were much lower than that of the other groups. Additionally, there was no significant difference among the three groups (OH-RVC-MS group, the COOR group, and plain RVC group). It indicated that the COOH-RVC-MS group improved the safety profile of ropivacaine as it was released at a constant and slow rate. Therefore, considering the safety perspective, COOH-RVC-MS group would be the priority. Furthermore, it was worth mentioning that there was significant distinction of administration dosages, routes as well as therapy duration in different clinical indications. Hence, the advantages and disadvantages of ropivacaine loaded microspheres prepared by different terminal groups on various indications should be explored deeply in the further.

4. Conclusion

In this study, PLGA with OH, COOH and COOR terminal groups were used to encapsulating ropivacaine as the matrix. Based on the narrow particle size distribution obtained by premix membrane emulsification, it was found that different terminal groups significantly affected the character of ropivacaine loaded microspheres, especially for encapsulation efficiency and *in vitro* release kinetics. Thereinto, the COOH-RVC-MS exhibited the highest encapsulation efficiency and slowest *in vitro* release profile whereas the COOR-RVC-MS showed lowest encapsulation efficiency and fastest release profile. According to the microcosmic analysis by QCM-D, AFM technique and confocal laser scanning microscopy, the COOH-PLGA exhibited a stronger absorption ability than that of OH-PLGA and COOR-PLGA. Hence, we attributed this distinction to the interactions between terminal groups and ropivacaine. In the meanwhile, the reaction activation centers of ropivacaine and PLGA molecules were identified by Density Functional and Frontier Molecular

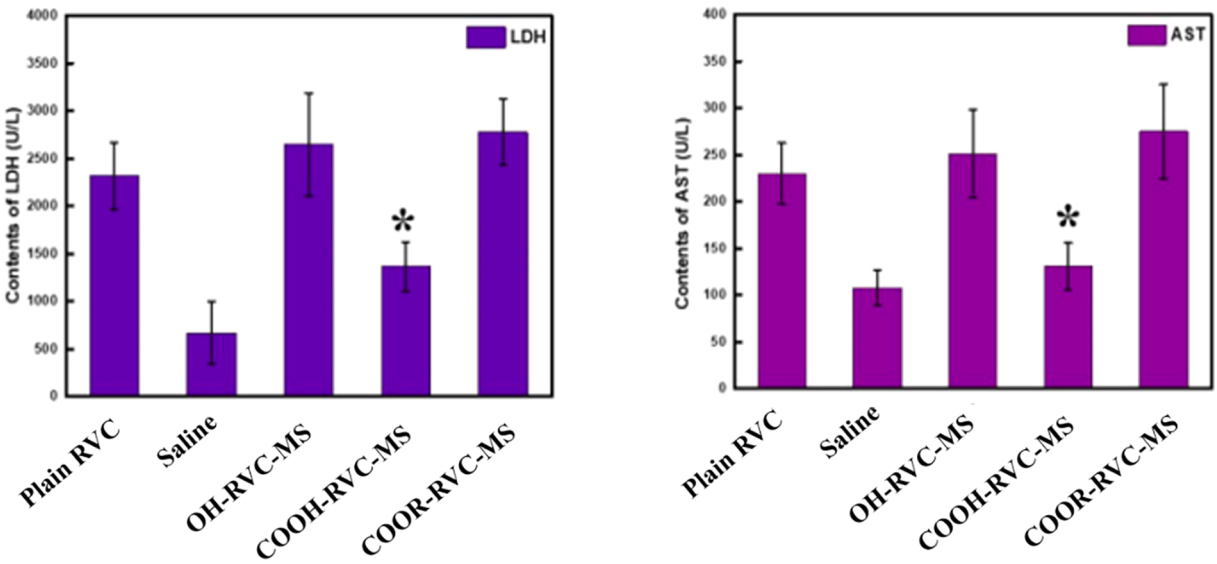

Fig. 9. The serum biochemical analysis on the cardiotoxicity of all formulations.

Orbits Calculations. The specific binding ability was verified at the molecular level. Additionally, *in vivo* release behavior of ropivacaine loaded microspheres fabricated by different terminal groups was compared in pharmacokinetic study. Combine with $T_{1/2}$, AUC, and MRT, the best- sustained release ability was exhibited in the OH-RVC-MS group. Furthermore, the pharmacodynamic evaluation was performed on rats of local infiltration model, according to the test of cutaneous trunci muscle. The results indicated that OH-RVC-MS group showed the best long-acting anesthetic effect, in terms of both intensity and duration. Finally, biochemical analysis results demonstrated that cardiotoxicity was significantly reduced by encapsulating ropivacaine into COOH-PLGA because of steady and slow release behavior *in vivo*.

This study provides novel insights on drug encapsulation mechanism which greatly contribute to designing PLGA based long acting formulation. Moreover, considering the administration dosage, regimens as well as safety issues, ropivacaine loaded microsphere prepared by different terminal groups of PLGA can be selected flexibly in terms of various indications in clinical.

Declaration of Competing Interest

The authors declare that they have no known competing financial interests or personal relationships that could have appeared to influence the work reported in this paper.

Acknowledgements

This work was supported by the National Key Technology Program (2017ZX09201004014), National Natural Science Foundation of China (NO. 21336010) and the National Key Research and Development Program of China (NO.2017YFC0210303).

Appendix A. Supplementary material

Supplementary data to this article can be found online at https://doi.org/10.1016/j.ejpb.2021.01.015.

References

[1] D.N. Kapoor, A. Bhatia, R. Kaur, R. Sharma, G. Kaur, S. Dhawan, PLGA: a unique polymer for drug delivery, Therapeutic Deliv. 6 (2015) 41–58.
[2] H.K. Makadia, S.J. Siegel, Poly Lactic-co-Glycolic Acid (PLGA) as Biodegradable Controlled Drug Delivery Carrier, Polymers 3 (2011) 1377.
[3] X. Hu, J. Zhang, X. Tang, M. Li, S. Ma, C. Liu, Y. Gao, Y. Zhang, Y. Liu, F. Yu, An Accelerated Release Method of Risperidone Loaded PLGA Microspheres with Good IVIVC, Curr. Drug Deliv. 14 (2017) -.
[4] A.C. Doty, D.G. Weinstein, K. Hirota, K.F. Olsen, R. Ackermann, W. Yan, S. Choi, S. P. Schwendeman, Mechanisms of in vivo release of triamcinolone acetonide from PLGA microspheres, J. Control. Release 256 (2017) 19–25.
[5] P. Blasi, A. Schoubben, S. Giovagnoli, L. Perioli, M. Ricci, C. Rossi, Ketoprofen poly (lactide-co-glycolide) physical interaction, Aaps Pharmscitech 8 (2007) E78–E85.
[6] Maria Manuela Gaspar, Dolores Blanco, Maria Eugénia M. Cruz, Formulation of L-asparaginase-loaded poly(lactide-co-glycolide) nanoparticles: influence of polymer properties on enzyme loading, activity and in vitro release, Journal of Controlled Release, 52 (1998) 53–62.
[7] Xanthe M. Lama*, Eileen T. Duenasa, Ann L. Daughertya, Nancy Levinb, a Jeffrey L. Cleland. Sustained release of recombinant human insulin-like growth factor-I for treatment of diabetes, Journal of Controlled Release, 67 (2000) 281–292.
[8] D.W. Choromanski, P.S. Patel, J.M. Frederick, S.E. Lemos, E.J. Chidiac, The effect of continuous interscalene brachial plexus block with 0.125% bupivacaine vs 0.2% ropivacaine on pain relief, diaphragmatic motility, and ventilatory function, J. Clin. Anesth. 27 (2015) 619–626.
[9] H. Zhang, Y. Lu, G. Zhang, S. Gao, D. Sun, Y. Zhong, Bupivacaine-loaded biodegradable poly(lactic- co -glycolic) acid microspheres : I. Optimization of the drug incorporation into the polymer matrix and modelling of drug release, Int. J. Pharm. 351 (2008) 244–249.
[10] J. Wu, Q. Fan, Y. Xia, G. Ma, J. Wu, Q. Fan, Y. Xia, G. Ma, Uniform-sized particles in biomedical field prepared by membrane emulsification technique, Chem. Eng. Sci. 125 (2015) 85–97.
[11] M. Bragagni, M.E. Gil-Alegre, P. Mura, M. Cirri, C. Ghelardini, L.D.C. Mannelli, Improving the therapeutic efficacy of prilocaine by PLGA microparticles: Preparation, characterization and in vivo evaluation, Int. J. Pharm. 547 (2018) 24.
[12] J.I. Tzeng, J.N. Wang, J.J. Wang, Y.W. Chen, C.H. Hung, Intrathecal rimantadine induces motor, proprioceptive, and nociceptive blockades in rats, Neurosci. Lett. 618 (2016) 94–98.
[13] X. Li, Y. Wei, P.P. Lv, Y.B. Wu, K. Ogino, G.H. Ma, Preparation of ropivacaine loaded PLGA microspheres as controlled-release system with narrow size distribution and high loading efficiency, Colloid Surf. A-Physicochem. Eng. Asp. 562 (2019) 237–246.
[14] Q. Feng, L. Yang, J. Wu, G. Ma, Z. Su, Microcosmic Mechanism of Dication for Inhibiting Acylation of Acidic Peptide, Pharm Res 32 (2015) 2310–2317.
[15] E.A. Yates, C.J. Terry, C. Rees, T.R. Rudd, L. Duchesne, M.A. Skidmore, R. Lévy, N. T.K. Thanh, R.J. Nichols, D.T. Clarke, Protein-GAG interactions: new surface-based techniques, spectroscopies and nanotechnology probes, Biochem. Soc. Trans. 34 (2006) 427–430.
[16] W. Yi, W. Yu Xia, W. Wei, S.V. Ho, Q. Feng, M. Guang Hui, S. Zhi Guo, Microcosmic mechanisms for protein incomplete release and stability of various amphiphilic mPEG-PLA microspheres, Langmuir 28 (2012) 13984–13992.
[17] L. Li, S.P. Schwendeman, Mapping neutral microclimate pH in PLGA microspheres, J. Control. Release 101 (2005) 163–173.
[18] B.J. Muller-Borer, H. Yang, S.A. Marzouk, J.J. Lemasters, W.E. Cascio, pHi and pHo at different depths in perfused myocardium measured by confocal fluorescence microscopy, Am. J. Physiol. 275 (1998) 1937–1947.
[19] A.B. Khodorova, G.R. Strichartz, The addition of dilute epinephrine produces equieffectiveness of bupivacaine enantiomers for cutaneous analgesia in the rat, Anesth. Analg. 91 (2000) 410–416.
[20] C.H. Hung, J.P. Shieh, C.C. Chiu, J.J. Wang, Y.W. Chen, Subcutaneous infiltration of doxylamine on cutaneous analgesia in rats, Pharmacol. Rep. 70 (2017) 565–569.

[21] B.T. Wu, K.T. Chen, K.S. Liu, Y.W. Chen, C.H. Hung, J.J. Wang, Clonidine intensifies memantine cutaneous analgesia in response to local skin noxious pinprick in the rat, Pharmacol. Rep. 67 (2015) 485–489.
[22] K. El-Boghdadly, A. Pawa, K.J. Chin, Local anesthetic systemic toxicity: current perspectives, Local Reg. Anesthesia 11 (2018) 35–44.
[23] A.P. Schwoerer, S. Hanno, F. Patrick, A Comparative Analysis of Bupivacaine and Ropivacaine Effects on Human Cardiac SCN5A Channels, Anesth. Analg. 120 (2015) 1226.
[24] H. Tsuchiya, M. Mizogami, T. Ueno, K. Shigemi, Cardiotoxic local anesthetics increasingly interact with biomimetic membranes under ischemia-like acidic conditions, Biol. Pharm. Bull. 35 (2012) 988–992.